Nonlinear Dyn (2019) 97:2579–2594
https://doi.org/10.1007/s11071-019-05149-5

ORIGINAL PAPER

Periodogram estimation based on LSSVR-CCPSO compensation for forecasting ship motion

Ming-Wei Li · Jing Geng · Wei-Chiang Hong · Li-Dong Zhang

Received: 4 March 2019 / Accepted: 15 July 2019 / Published online: 25 July 2019
© Springer Nature B.V. 2019

Abstract A ship motion time series (SMTS) exhibits obvious periodicity under the effects of periodic wave and strong nonlinearity owing to wind, ocean currents, and the load of ship itself, which make accurate forecasting difficult. To improve forecasting accuracy, this investigation divides the SMTS into a periodic term and a nonlinear term and forecasts each term separately. First, the periodogram estimation method (PEM) is implemented to forecast the periodic term. Then, owing to the strong nonlinearity of SMTS, the LSSVR model is used to forecast the nonlinear residual term that is generated by the PEM. On account of parameters that determine the predictive accuracy of the LSSVR model, the chaotic cloud particle swarm optimization (CCPSO) algorithm is introduced to optimize the parameters of the LSSVR model. Finally, combining the PEM, LSSVR model, and CCPSO algorithm, a hybrid forecasting method for SMTS, PEM&LSSVR-CCPSO, is developed. Subsequently, SMTS data for two ships that are sailing on the ocean are used as a numerical example, and thus, the forecasting performance of the presented method is evaluated. The results of the analysis demonstrate that the proposed hybrid SMTS forecasting scheme has better forecasting performance than classical forecasting models that are considered herein.

Keywords Ship motion time series forecast · Periodogram estimation method (PEM) · Least squares support vector regression (LSSVR) · Chaos theory · Cloud model · Particle swarm optimization (PSO)

M.-W. Li · J. Geng · L.-D. Zhang
College of Shipbuilding Engineering, Harbin Engineering University, Harbin 150001, Heilongjiang, China
e-mail: limingwei@hrbeu.edu.cn

J. Geng
e-mail: gengjing@hrbeu.edu.cn

L.-D. Zhang
e-mail: zhanglidong@hrbeu.edu.cn

W.-C. Hong (✉)
School of Computer Science and Technology, Jiangsu Normal University, Xuzhou 221116, China
e-mail: hongwc@jsnu.edu.cn

1 Introduction

When sailing, a ship exhibits six degree-of-freedom motion under the effects of waves, currents, winds, and the load of ship itself. SMTS can be forecast to guide ship-borne aircrafts in taking off and landing on deck, optimizing the turning time of the ship in wind and waves, improving the accuracy of launched missiles, positioning mine hunting boats, and providing a basis for decision making in the course of navigation. Therefore, the accurate forecasting of SMTS has important military significance and civil value.

Numerous papers on SMTS forecasting have been published. The periodogram estimation method, the grey system theory prediction method, the time series analysis method, and the intelligent forecasting method

have been applied to forecast SMTS. SMTS exhibits strong periodicity under the action of periodic waves, so the PEM can be used in forecasting SMTS to deal effectively with the periodicity of SMTS [1]. However, PEM cannot handle the nonlinearity of SMTS. Owing to the insufficiency of PEM, its ability to solve nonlinear problems is improved using the data intersection segmentation and windowed window function [2]. Nevertheless, as the ship's speed decreases, or the sea conditions become more complicated, the nonlinearity of its motion increases, making difficult accurate forecasting of SMTS even by the improved PEM. Shen [3] was the first to apply grey system theory (GM) to SMTS forecasting, and then Liu and Peng [4] used the second-order grey neural network model to forecast the SMTS. These works have improved forecasting accuracy, but a data series that is modeled by GM must be described by a discrete function and be smooth, and these conditions are unlikely to be satisfied by SMTS with strong nonlinearity. Accordingly, the GM method is very limited in SMTS forecasting. Yumori [5] presented an SMTS forecasting method that was based on the ARMA model, which involves a simple modeling process, but the forecasting step length was only 2 to 4 s. Zhang et al. [6] and Zhao et al. [7], respectively, used the AR model and the ARMA model to forecast SMTS and achieved more accurate forecasting. Peng and Liu [8] used the lattice recursive least squares algorithm to improve the AR model and established a novel parameter estimation method for the AR model, improving its forecasting accuracy and increasing its calculation speed. However, both AR and ARMA models assume linearity, limiting their (application to OR use in) SMTS forecasting on account of its strong nonlinearity.

To overcome the nonlinearity of SMTS, artificial neural network (ANN) models, which are very effective in strongly nonlinear processing, have been successfully used in SMTS forecasting. Khan et al. [9] used the ANN model to forecast SMTS and obtained excellent forecasting performance with a forecasting step of up to 7 s. Gu et al. [10] used the chaotic mapping mechanism and the RBFNN model to develop a new SMTS forecasting approach, which achieved a forecasting accuracy of 85% with a forecast step length of up to 10 s. Shen and Xie [11] and Xu et al. [12], respectively, presented SMTS forecasting models that were based on the ANN model and the diagonal regressive neural network and obtained more accurate forecasts. Although ANNs have been widely used in SMTS forecasting, they have inherent shortcomings. For experienced risk minimization, model training of the ANN depends on the use of enough samples, but too many samples lead to over-fitting. Furthermore, the operations of an ANN are also difficult to explain and ANNs easily fall into local optima.

For structure risk minimization, support vector regression (SVR) can overcome the local minima, over-learning and dimension disaster problems of the ANN [13]. SVR-based models [14] have been used in numerous fields, including tourism forecasting [15], traffic flow forecasting [16], and port throughput forecasting [17]. Previous investigations [17–19] have presented various forecasting methods based on the SVR-based model, and numerical experiment results have demonstrated that the proposed SVR-based models have better forecasting performance than that of forecasting models that are based on an ANN. Recently, Li et al. [20] have developed an SVR-based model for the more accurate forecasting SMTS and obtained forecasting results, improving the accuracy of forecasting SMTS. However, SMTS has strong periodic characteristics under the action of periodic waves, so even though the SVR-based model is effective for nonlinear processing, it cannot handle the periodicity of SMTS, which limits its application to SMTS forecasting.

In summary, in the course of navigation and the operation of ship motion, the action of periodic waves, wind, ocean currents, and the load of ship itself, SMTS exhibits obvious periodic characteristics and strong nonlinearity. Accurately forecasting SMTS using a single nonlinear model is difficult. Additionally, owing to the strong periodic characteristics of SMTS, forecasting using nonlinear models is also difficult. The periodic forecasting model can effectively overcome the periodic characteristics of SMTS, but it cannot handle the randomness or nonlinearity in SMTS. Briefly, neither a single nonlinear model nor a periodic forecasting model can simultaneously deal with the periodic characteristics and nonlinearity of SMTS.

To improve the accuracy of forecasting SMTS, given both the periodicity and the nonlinearity of SMTS, the SMTS is divided into a periodic term and a nonlinear term; the PEM and LSSVR models are combined to forecast these two terms separately, and a coupled forecasting approach is developed. In view of the periodic processing ability of PEM [1], PEM is utilized herein to simulate the periodic characteristics of SMTS and forecast its periodic term. Then, owing to the excellent

performance of the LSSVR model in SMTS forecasting [19], the LSSVR model is used to forecast the residual term of SMTS that is generated by PEM, and to forecast the nonlinear term.

Since the optimization of parameters influences the forecasting accuracy of the LSSVR model, Li and his colleagues established a series of SVR-based forecasting approaches by hybridizing an SVR model with various improved evolutionary algorithms [16,19–21]. In recent years, several novel effective global optimization strategies have been developed to address engineering optimization problems [22–24], and they have the potential to be used to optimize the parameters of the LSSVR model. In particular, the CCPSO algorithm, which uses a chaotic mapping function to increase the diversity of a population over the whole searching space and uses cloud theory to select parameters carefully, has been proposed [25]; it performs well in optimizing classical functions. Therefore, to find an effective combination of parameters of the LSSVR model, this work introduces CCPSO to optimize the combination of parameters of the LSSVR model.

For the above reasons, a hybrid method for forecasting SMTS was proposed: the periodic term is forecast by PEM; the residual term is forecast using the LSSVR model, and the parameters of the LSSVR model are determined by CCPSO. To evaluate both feasibility and superiority, numerical experiments were performed with SMTS data for two ships that are sailing on the ocean. The PEM, BPNN, LSSVR-CCPSO, PEM&BPNN, and PEM&LSSVR-CCPSO approaches were used and their forecasting accuracies tested, and then the parameter optimization performances of GA, PSO, FOA, BA, and CCPSO are all analyzed.

The rest of this article is organized as follows. Section 2 presents the PEM for forecasting the periodic term, the LSSVR-CCPSO method for forecasting the residual term, and CCPSO method for determining the parameters of the LSSVR model. Section 3 presents numerical experiments. Finally, Sect. 4 draws brief conclusions.

2 PEM&LSSVR-CCPSO model

2.1 Construction of PEM&LSSVR-CCPSO model

Since handling both the periodicity and the strong nonlinearity of SMTS using only a nonlinear model or the periodogram method, this work attempts to hybridize the periodogram method with the LSSVR model to develop a coupled SMTS forecasting method. The PEM is used to handle the periodic characteristics of SMTS and to forecast the periodic term, $Y_{\text{periodic}}(n)$. Owing to its excellent performance in dealing with nonlinear problems [19], the LSSVR model is used to forecast the residual term of the regression sequence of the PEM, $Y_{\text{residual}}(n)$. Then, the forecast SMTS values, $Y(n)$, are given by Eq. (1),

$$Y(n) = Y_{\text{periodic}}(n) + Y_{\text{residual}}(n) \tag{1}$$

where $Y(n)$ is forecast value for the nth time point; $Y_{\text{periodic}}(n)$ is the periodic term of $Y(n)$; $Y_{\text{residual}}(n)$ is the residual term of $Y(n)$; $n = 1, 2, \ldots, N$, $N$is the number of the sample.

The method for forecasting $Y_{\text{periodic}}(n)$ and $Y_{\text{residual}}(n)$ is described as follows.

2.2 Forecasting periodic term by PEM

An SMTS is a typical stationary random sequence of values that are obtained from a real environment with a strong correlation and periodicity, so it can be described using a series of periodic terms and a stationary random sequence. The PEM uses SMTS data that are collected to estimate the periodic term and make an approximate forecast. The periodic term, $Y_{\text{periodic}}(n)$, of an SMTS is given by Eq. (2),

$$Y_{\text{periodic}}(n) = P(n) + Z(n) \tag{2}$$

where $P(n)$ is the periodic term; $Z(n)$ is stationary random sequences with zero mean.

The ship motion system is a zero-mean system, so the stationary random sequence term, $Z(n)$, is zero. Accordingly, in the process of forecasting ship motion based on the PEM, the periodic term is considered, and $Z(n)$ does not have to be estimated. To simplify the problem, suppose $P(n)$ is a harmonic function, as in Eq. (3),

$$Y_{\text{periodic}}(n) = P(n) = ae^{j\omega_1 nT} \tag{3}$$

where T is the sampling period; nT is the sampling time; ω_1 is the harmonic angular frequency; a is the amplitude; $|a|$ is the harmonic amplitude; $\angle a$ is the initial phase angle of the harmonics. Equation (4) is the matrix form of Eq. (3):

$$\begin{bmatrix} Y_{\text{periodic}}(1) \\ Y_{\text{periodic}}(2) \\ \vdots \\ Y_{\text{periodic}}(N) \end{bmatrix} = \begin{bmatrix} e^{j\omega_1 T} \\ e^{j\omega_1 2T} \\ \vdots \\ e^{j\omega_1 NT} \end{bmatrix} a \tag{4}$$

This equation can be simply stated as Eq. (5):

$$Y = \Phi a \tag{5}$$

The problem is simplified to that of calculating $\hat{a}$ and $\hat{\omega}_1$ of a and ω_1 and to minimize the objective function J, as in Eq. (6),

$$J = \left(Y - \hat{\Phi}\hat{a}\right)^{\mathrm{T}} \left(Y - \hat{\Phi}\hat{a}\right) \tag{6}$$

Based on the obtained $\hat{\omega}_1$, $\hat{\Phi}^{\mathrm{T}}$ is calculated using Eq. (7):

$$\hat{\Phi}^{\mathrm{T}} = \left[e^{-j\hat{\omega}_1 T} e^{-j\hat{\omega}_1 2T} \cdots e^{-j\hat{\omega}_1 NT}\right] \tag{7}$$

Then, the least squares method is used to obtain the least squares estimate, $\hat{a}_1$, of a, using Eq. (8),

$$\hat{a}_1 = \left(\hat{\Phi}^{\mathrm{T}}\hat{\Phi}\right)^{-1} \left(\hat{\Phi}^{\mathrm{T}} Y\right) \tag{8}$$

Then, J can be re-written as Eq. (9),

$$\begin{aligned} J &= \left(Y - \hat{\Phi}\hat{a}\right)^{\mathrm{T}} \left(Y - \hat{\Phi}\hat{a}\right) = \left[\left(Y - \hat{\Phi}\hat{a}_1\right)\right. \\ &\quad \left. - \left(\hat{\Phi}\hat{a} - \hat{\Phi}\hat{a}_1\right)\right]^{\mathrm{T}} \left[\left(Y - \hat{\Phi}\hat{a}_1\right) - \left(\hat{\Phi}\hat{a} - \hat{\Phi}\hat{a}_1\right)\right] \\ &= \left(Y - \hat{\Phi}\hat{a}_1\right)^{\mathrm{T}} \left(Y - \hat{\Phi}\hat{a}_1\right) \\ &\quad + \left(\hat{\Phi}\hat{a} - \hat{\Phi}\hat{a}_1\right)^{\mathrm{T}} \left(Y - \hat{\Phi}\hat{a}_1\right) \\ &\quad + \left(\hat{a} - \hat{a}_1\right)^{\mathrm{T}} \hat{\Phi}^{\mathrm{T}}\hat{\Phi}\left(\hat{a} - \hat{a}_1\right) \end{aligned} \tag{9}$$

where $\left(\hat{\Phi}\hat{a} - \hat{\Phi}\hat{a}_1\right)^{\mathrm{T}} \left(Y - \hat{\Phi}\hat{a}_1\right) = \left(\hat{a} - \hat{a}_1\right)^{\mathrm{T}} \hat{\Phi}^{\mathrm{T}}\hat{Y} = 0$, and therefore, the problem can be briefly stated as Eq. (10),

$$\mathrm{Min} J_1 = \left(Y - \hat{\Phi}\hat{a}_1\right)^{\mathrm{T}} \left(Y - \hat{\Phi}\hat{a}_1\right) \tag{10}$$

Substituting Eq. (8) into Eq. (10) yields Eq. (11):

$$\begin{aligned} \mathrm{Min} J_1 &= \left[Y - \hat{\Phi}\left(\hat{\Phi}^{\mathrm{T}}\hat{\Phi}\right)^{-1} \hat{\Phi}^{\mathrm{T}} Y\right]^{\mathrm{T}} \\ &\quad \times \left[Y - \hat{\Phi}\left(\hat{\Phi}^{\mathrm{T}}\hat{\Phi}\right)^{-1} \hat{\Phi}^{\mathrm{T}} Y\right] \\ &= Y^{\mathrm{T}} Y - Y^{T}\hat{\Phi}\left(\hat{\Phi}^{\mathrm{T}}\hat{\Phi}\right)^{-1} \hat{\Phi}^{\mathrm{T}} Y \end{aligned} \tag{11}$$

From Eq. (7), Eqs. (12)–(14) are obtained:

$$\begin{aligned} \hat{\Phi}^{\mathrm{T}}\hat{\Phi} &= \left[e^{-j\hat{\omega}_1 T}\ e^{-j\hat{\omega}_1 2T}\ \cdots\ e^{-j\hat{\omega}_1 NT}\right] \\ &\quad \times \begin{bmatrix} e^{-j\hat{\omega}_1 T} \\ e^{-j\hat{\omega}_1 2T} \\ \vdots \\ e^{-j\hat{\omega}_1 NT} \end{bmatrix} = N \end{aligned} \tag{12}$$

$$\hat{\Phi}^{\mathrm{T}} Y = \sum_{i=1}^{N} e^{-j\hat{\omega}_1 iT} Y(i) \tag{13}$$

$$\mathrm{Y}^{\mathrm{T}}\hat{\Phi} = \sum_{i=1}^{N} e^{-j\hat{\omega}_1 iT} Y(i) \tag{14}$$

Substituting Eqs. (12)–(14) into Eq. (11) converts the problem of minimizing J_1 into Eq. (15),

$$\mathrm{Min} J_1 = \sum_{i=1}^{N} |Y(i)|^2 - \frac{1}{N}\left|\sum_{i=1}^{N} e^{-j\hat{\omega}_1 iT} Y(i)\right|^2 \tag{15}$$

Clearly, this problem is equivalent to Eq. (16):

$$\mathrm{Max} J_2 = \frac{1}{N}\left|\sum_{i=1}^{N} e^{-j\hat{\omega}_1 iT} Y(i)\right|^2 \tag{16}$$

The periodogram of $P(n)$, $I_n(\omega_1)$, satisfies Eq. (17):

$$I_n(\omega_1) \triangleq \frac{1}{N}\left|\sum_{i=1}^{N} e^{-j\hat{\omega}_1 iT} Y(i)\right|^2 \tag{17}$$

where $\hat{\omega}_1$ is the least square estimator of ω_1 that maximizes $I_n(\omega_1)$.

Substituting $\hat{\omega}_1$ into Eqs. (7) and (8) yields $\hat{\Phi}$ and the $\hat{a}_1$, respectively. Then, substituting these parameters into Eq. (3) yields $P(n)$. Similarly, all of the periodic terms are calculated.

Eventually, the forecasting of the periodic term, $P(n)$, using the PEM, proceeds as follows.

First, calculate the period diagram, $I_n(\omega_1)$, of $P(n), n = 1, 2, \ldots, N$, as in Eq. (18). Let $\omega_1 \triangleq \omega_{k1} = \frac{2k\pi}{NT_1}, k = 0, 1, \ldots, M$, for various ω_{k1}, and compare the size of $I_n(\omega_{k1})$. When $I_n(\omega_{k^*1}) = \max_{1\le k1\le N}\{I_n(\omega_{k1})\}$, let $\omega_1 = \omega_{k^*1}$ be the angular frequency of the first periodic term of the SMTS.

Second, use the least squares method to obtain the least squares estimators, $\hat{a}_1$ and $\hat{\omega}_1$ of a_1 and ω_{k^*1}, respectively, where $\hat{\Phi}^{\mathrm{T}} = \left[e^{-j\hat{\omega}_1 T_1}\ e^{-j\hat{\omega}_1 2T_1}\ \cdots\ e^{-j\hat{\omega}_1 NT_1}\right]$.

Third, the first periodic term is obtained as Eq. (18):

$$P_{\text{periodic}}(1) = \hat{a}_1 e^{j\hat{\omega}_1 nT_1} \tag{18}$$

Fourth, if the SMTS contains a second periodic term, $P_{\text{periodic}}(2)$, then $\hat{a}_2$ and $\hat{\omega}_2$ can also be obtained using the above process, and it is then given by Eq. (19):

$$P_{\text{periodic}}(2) = \hat{a}_2 e^{j\hat{\omega}_2 n T_2} \tag{19}$$

Finally, all of the periodic items are obtained using the above method. The number of obtained periodic function items is assumed to be Q, and then the periodic term of the SMTS, $Y_{\text{periodic}}(n)$, is given by Eq. (20),

$$Y_{\text{periodic}}(n) = \sum_{q=1}^{Q} P_{\text{periodic}}(q) = \sum_{q=1}^{Q} \hat{a}_q e^{j\hat{\omega}_q n T_q} \tag{20}$$

where $P_{\text{periodic}}(q)$ is the qth periodic term of the SMTS.

2.3 Forecasting residual term using LSSVR-CCPSO

2.3.1 LSSVR modeling

In 1999, Suykens proposed LSSVR [26], which is a machine learning method that is based on statistical theory and criteria for minimizing structural risk. The inequality constraint is replaced by the equality constraint by taking the loss function and the error square as the empirical loss of the training set, and the quadratic programming problem is transformed into the problem of solving linear equations, increasing the calculation speed, convergence precision, and generalizability. In this investigation, the LSSVR model is used to forecast the residual error that is generated by the PEM. The forecasting principle of the LSSVR model is as follows.

The sample data are assumed to satisfy $X = \{x_i, y_i\}_{i=1}^{n}$, where $x_i \in \mathcal{R}^d$ is the input vector, $y_i \in \mathcal{R}$ is the output value, and n is the number of data samples. The nonlinear mapping function, $\varphi(x)$, is used to map the input space of the sample to the high-dimensional feature space. Then, the regression function is constructed as Eq. (21):

$$f(x) = \mathbf{w}^{\mathrm{T}} \varphi(x) + b \tag{21}$$

where b is the threshold and $\mathbf{w}^{\mathrm{T}}$ is the regression coefficient vector.

Unlike the traditional SVR model, the LSSVR model solves the minimization problems that satisfy Eq. (22),

$$\begin{aligned} \text{Min} U &= \frac{1}{2}\left\|w^2\right\| + C\sum_{i=1}^{n} e_i^2 \\ \text{s.t. } y_i - f(x_i) &= e_i \\ e_i &\geq 0 \end{aligned} \tag{22}$$

The Lagrange multiplier, α_i, is introduced to transform the optimization problem Eq. (22) into Eq. (23),

$$\begin{aligned} L(\omega, b, e_i, \alpha_i) = \frac{1}{2}\left\|w^2\right\| + C\sum_{i=1}^{n} e_i^2 \\ - \sum_{i=1}^{n} \alpha_i (e_i + f(x_i) - y_i) \end{aligned} \tag{23}$$

Equation (23) is used to obtain partial derivatives for w, b, e_i, and α_i, and under KKT (Karush–Kuhn–Tucker) optimal conditions, the following linear equation Eq. (24) is obtained.

$$\begin{bmatrix} 0 & \mathbf{I}' \\ \mathbf{IZ}\ \mathbf{Z}' + C^{-1}\mathbf{I} \end{bmatrix} \begin{bmatrix} b \\ \boldsymbol{\alpha} \end{bmatrix} = \begin{bmatrix} 0 \\ \mathbf{y} \end{bmatrix} \tag{24}$$

where $\mathbf{y} = [y_1, y_2, \ldots, y_n]$; $\mathbf{I} = [1, 1, \ldots, 1]'$; $\alpha = [\alpha_1, \alpha_2, \ldots, \alpha_n]$; and $\mathbf{Z} = [\varphi(x_1), \varphi(x_2), \ldots, \varphi(x_n)]$. The kernel function [27], $K(x_i, x_j)$, is introduced to prevent the dimensionality disaster, and its value is given by $K(x_i, x_j) = \varphi(x_i) \circ \varphi(x_j)$.

The most commonly used kernel functions are radial basis (RBF) kernel functions, sigmoid kernel functions, linear kernel functions, and polynomial kernel functions. The RBF kernel function can be adapted to randomly distributed samples by artificially selecting appropriate parameters, and it is the most widely used. Therefore, the RBF kernel function is used in this paper. Its specific form is given by Eq. (25),

$$K(x, y) = \exp\left(\frac{(x-y)^2}{2\sigma^2}\right) \tag{25}$$

where the σ is a parameter of a kernel function.

Then, the regression function of the LSSVR model is obtained as Eq. (26):

$$f(x) = \sum_{i=1}^{n} \alpha_i K(x_i, x) + b \tag{26}$$

The residual term of the SMTS, $Y_{\text{residual}}(n)$, is given by Eq. (27),

$$Y_{\text{residual}}(n) = f(x) = \sum_{i=1}^{n} \alpha_i K(x_i, x) + b \tag{27}$$

Based on the brief modeling process mentioned above, LSSVR involves two regularization parameters, which are C and the radial basis kernel function, σ. The forecasting performance of the LSSVR model is

strongly related to the selection of these two parameters: C and σ. The purpose of C is to balance the confidence range and the experience risk of learning machines. If C is too large, then the goal is only to minimize the experience risk. When the value of C is too small, the penalty associated with the experience error is small, increasing the experience risk. σ controls the width of the Gaussian function and the distribution range of the training data. A smaller σ indicates a greater structural risk, which results in over-fitting. Therefore, the selection of the LSSVR parameters has always been crucial to improving the accuracy of forecasting using the LSSVR model.

In traditional methods, the parameters of the LSSVR model are mainly determined by grid search and previous searching experiences. However, the computational complexity of the grid search method is large. Furthermore, these two methods are not guaranteed to find the global optimal solution. Since parameter optimization is one of the effective methods for improving the forecasting accuracy of the LSSVR model, it is also required to improve the fitting ability of LSSVR. Accordingly, LSSVR parameter optimization has always been a hot research topic.

2.3.2 Determination of parameters of LSSVR model by CCPSO

The authors of this investigation have published numerous studies of the optimization of the parameters of SVR-based models using evolutionary algorithms [16,19–21]. The results of these studies demonstrate that the forecasting accuracy of the SVR-based model can be improved by optimizing the parameters using the evolutionary algorithm. According to the literature [25], to overcome the easy falling into local extrema and the slow convergence in the late stages of the PSO algorithm, chaotic mapping and the cloud model are used. The CCPSO algorithm is proposed and yields better solutions than other algorithms. To determine better parameters of the LSSVR model, the CCPSO algorithm is used to optimize the parameters of the LSSVR model. The procedure for determining the parameters of the LSSVR model using the CCPSO algorithm is as follows.

Step 1 Parameter initialization Initialize the size of the particle swarm, *pop_size*; the maximal number of iterations, *gen_max*; the acceleration parameters, c_1 and c_2; the hybrid control parameter, *mix_gen*; and the population distribution coefficient, *pop_dist*.

Step 2 Population initialization Randomly generate *pop_size* particles, $g = \{g_1, g_2, \ldots, g_{pop\_size}$ in the feasible region $[g_{C\min}, g_{C\max}]$ and $[g_{\sigma}\min, g_{\sigma}\max]$, where $g_j = C_j, \sigma_j$. Let $G = 1, GG = 1$.

Step 3 Evaluation of fitness Use the vector $g_j = (C_j, \sigma_j)$ to provide the parameters of the LSSVR_j model; use the training data to train the LSSVR_j model; and calculate the regression value of the LSSVR_j model that is associated with the parameter C_j, σ_j. Then, the forecasting error (as the fitness value of the CCPSO) is calculated by the mean absolute percentage error (MAPE), as in Eq. (28).

$$\text{MAPE} = \frac{1}{n}\sum_{i=1}^{n}\left|\frac{f(x_i) - \hat{f}(x_i)}{f(x_i)}\right| \times 100\% \tag{28}$$

where n is the total number of data points; is the actual value at point i; and is the forecasted value at point i.

Step 4 Update the optimum Update the individual optimal position, P_i^G, and the global optimal position, P_g^G.

Step 5 The criterion of the maximal number of iterations If $G < gen\_max$, then go to *Step 6*; otherwise, go to *Step 8*.

Step 6 Calculate the inertia weight factor Calculate the adaptive inertia weight factor, ω, using Eq. (29) [28]. Update the speed and position of each particle in the particle swarm, and then set $G = G + 1$ and $GG = GG + 1$, and go to *Step 7*.

$$\omega = \begin{cases} \omega_{\min} & f_i > \bar{f}_{\text{good}} \\ \omega_{\min} + (\omega_{\max} - \omega_{\min})\frac{\bar{f}_{\text{good}} - f_i}{\bar{f}_{\text{good}} - \bar{f}_{\text{bad}}} & \bar{f}_{\text{bad}} \le f \le \bar{f}_{\text{good}} \\ \omega_{\max} & f_i < \bar{f}_{\text{bad}} \end{cases} \tag{29}$$

where ω is the updated weight; f_i is the fitness value of the ith particle; $\bar{f}_{\text{good}}$ is the mean fitness value of a particle that is superior to the mean fitness value $\bar{f}$ of the particle swarm; $\bar{f}_{\text{bad}}$ is the mean fitness value of a particle that is inferior to the mean fitness value $\bar{f}$ of the particle swarm; $\omega_{\min}$ and $\omega_{\max}$ and are, respectively, the minimum and maximum values of the inertia weight, 0.4 and 0.9.

Step 7 The criterion of the hybrid control condition If $GG < mix\_gen$, then go to *Step 3*; otherwise, go to *Step 8*.

Step 8 Chaotic global exploration and cloud local accelerated search Take the individual optimal position, P_i^G, of each particle to form a new swarm and

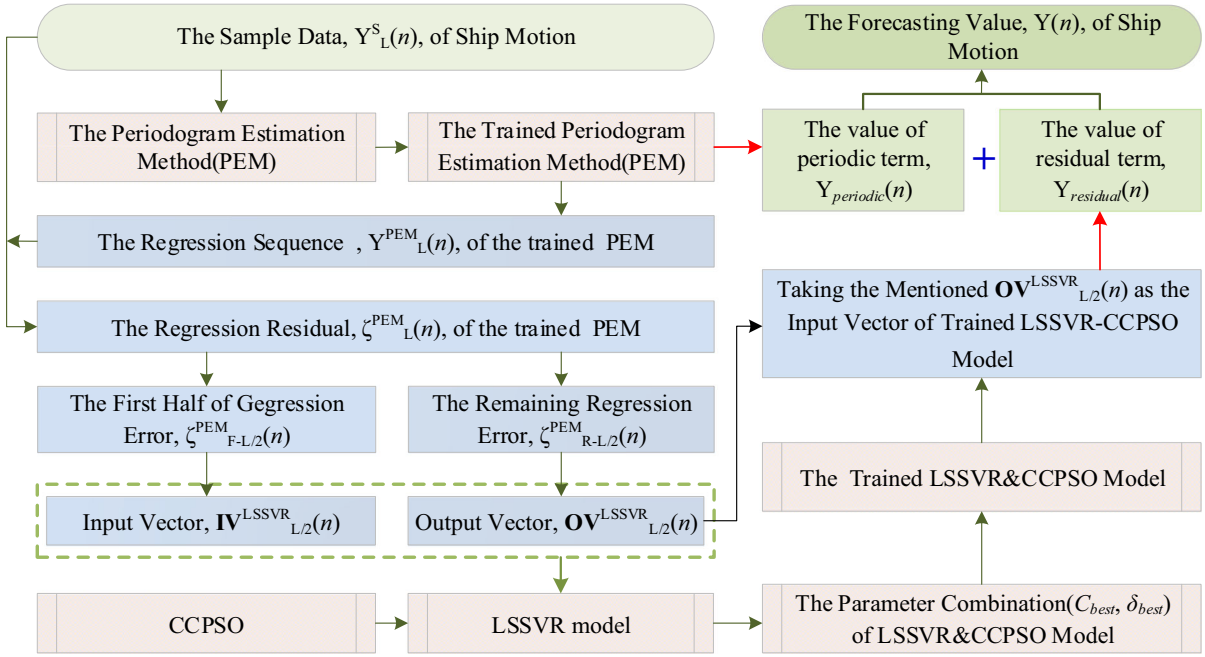

Fig. 1 The forecasting flowchart of the PEM&LSSVR-CCPSO model

sequence based on the fitness value of the *i*th particle; divide the whole swarm into *pop_distr*pop_size* better individuals and *(1-pop_distr)*pop_size* poorer individuals. For the *pop_distr*pop_size* better individuals, perform a local search with the cloud model, and obtain *pop_distr*pop_size* new better individuals [25]. For the (1-*pop_distr*)**pop_size* poorer individuals, execute a global chaotic disturbance with the cat mapping function obtain (1-*pop_distr*)**pop_size* new better individuals [25]. Consolidate the *pop_distr*pop_size* new better individuals and the (1-*pop_distr*)**pop_size* new poorer individuals to generate a new elite swarm. Let $GG = 0$, and go to *Step 3*.

Step 9 Parameter determination Take the global optimal position, P_g^G, of the current population as the parameters of the LSSVR model.

2.4 Implementation of PEM&LSSVR-CCPSO method

Consistent with the forecasting principle of the PEM and the LSSVR model, first L sample data are used to train the PEM; the regression value of the PEM is calculated; $Y_{\text{periodic}}(n)$ is predicted; and the regression residual error of the trained PEM is computed. Then, the obtained regression residual error is used as the input and output vectors of the LSSVR model; CCPSO is used to optimize the LSSVR-CCPSO model, and $Y_{\text{residual}}(n)$ is forecast. Finally, $Y_{\text{periodic}}(n)$ and $Y_{\text{residual}}(n)$ are summed to yield the forecast value, $Y(n)$.

Figure 1 displays the details of the following forecasting process.

Step 1 Use the L sample data, $Y^S_{L(n)}$, to train the PEM.

Step 2 Use the trained PEM to calculate the regression sequence, $Y^{\text{PEM}}_{L(n)}$, and forecast the value of the periodic term, $Y_{\text{periodic}}(n)$, of the SMTS.

Step 3 Using the regression sequence, $Y^{\text{PEM}}_{L(n)}$, and sample data, $Y^S_{L(n)}$, calculate the regression residual, $\zeta^{\text{PEM}}_{L(n)}$.

Step 4 Take the first half of the regression error, $\zeta^{\text{PEM}}_{F-\frac{L}{2}(n)}$, as the input vector, $\text{IV}^{LSSVR}_{\frac{L}{2}(n)}$, and the remaining part of the regression error, $\zeta^{\text{PEM}}_{R-\frac{L}{2}(n)}$, as the output vector, $\text{OV}^{\text{LSSVR}}_{\frac{L}{2}(n)}$, of the LSSVR model.

Step 5 Using $\text{IV}^{\text{LSSVR}}_{\frac{L}{2}(n)}$ and $\text{OV}^{\text{LSSVR}}_{\frac{L}{2}(n)}$, use the CCPSO to determine the parameters of the LSSVR model, $(C_{\text{best}}, \sigma_{\text{best}})$.

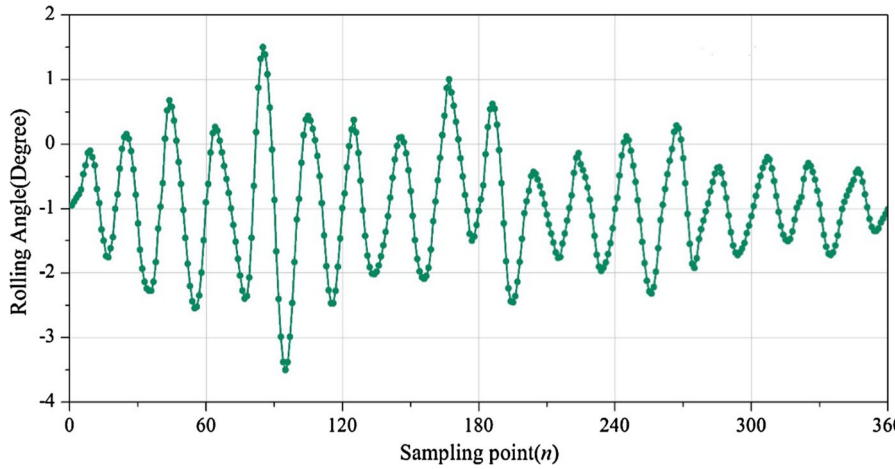

Fig. 2 Data distribution of Example I

Step 6 Train the LSSVR model with $(C_{\text{best}}, \sigma_{\text{best}})$ to obtain the trained LSSVR-CCPSO model; then take the aforementioned $\text{OV}_{\frac{L}{2}(n)}^{\text{LSSVR}}$ as the input vector of the trained LSSVR-CCPSO model, and forecast the value of the residual term, $Y_{\text{residual}}(n)$, of the SMTS.

Step 7 Add the value of the residual term, $Y_{\text{residual}}(n)$ to the value of the periodic term, $Y_{\text{periodic}}(n)$ to obtain the final forecast value, $Y(n)$, of the SMTS.

3 Experimental examples

3.1 Dataset of numerical examples

To test the feasibility and universal applicability of the proposed PEM&LSSVR-CCPSO model, SMTS data for two ships that were sailing on the ocean are used to make a numerical forecast. In Example I, the sea condition is 2, the ship speed is 20 knots, and the ship has a bearing of 115°. In Example II, the sea condition is 4; the ship speed is 15 knots, and the ship has a bearing of 145°. With 0.5 s as the sampling interval, each example comprises 360 SMTS data samples.

The SMTS data are divided into two subsets. The first 320 SMTS values are selected as the training set, so the training parameter, L, is 320; the other 40 SMTS values are used as the testing set. Figures 2 and 3 present the SMTS values in Examples I and II .

Since using sample data to train directly the forecasting model may lead to neurons appear saturation phenomenon, the sample data must be normalized to ensure that they are within a certain interval ([0,1] herein) and of the same order of magnitude.

The SMTS data are normalized according to Eq. (30),

$$y_i = \frac{x_i - \min(x_i)}{\max(x_i) - \min(x_i)} \tag{30}$$

where x and y, respectively, are the values before and after the normalization of sample data; $\min(x_i)$ and $\max(x_i)$, respectively, represent the maximum and minimum values of sample data; and $i = 1, 2, \ldots, Q$ (where Q is the number of samples).

After the forecasting, inverse normalization, Eq. (31), must be used to calculate the actual SMTS values:

$$x_i = [\max(x_i) - \min(x_i)]\, y_i + \min(x_i) \tag{31}$$

3.2 Forecasting accuracy evaluation index

In testing the feasibility and effectiveness of the CCPSO algorithm in determining the parameters of the LSSVR model, the MAPE, mentioned above Eq. (28), and the root mean square error (RMSE) are used as indices of the forecasting performance of each model. The RMSE is given by Eq. (32),

$$\text{RMSE} = \sqrt{\frac{\sum_{i=1}^{n} \left(f(x_i) - \hat{f}(x_i)\right)^2}{n}} \tag{32}$$

where n is the total number of data points; $f(x_i)$ is the actual SMTS value at point i; and $\hat{f}(x_i)$ is the forecasted SMTS value at point i.

3.3 Parameter setting

Experience has shown that the settings of the parameters of a model significantly affect its forecasting accuracy.

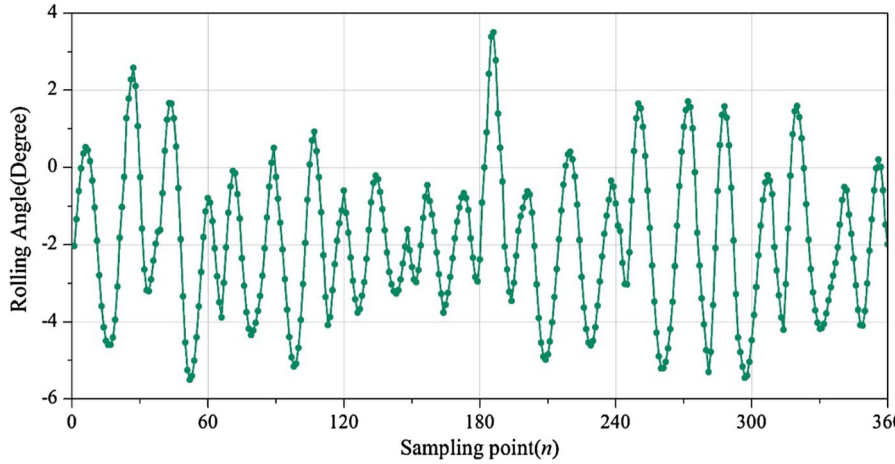

Fig. 3 Data distribution of Example II

The parameters of the selected optimization algorithm and the forecasting models are set as follows. The parameters of the BPNN, GA, FOA, BA, PSO, and CCPSO and the feasible regions of the parameters of the LSSVR model for forecasting SMTS are obtained by trial calculation using data from two examples.

(1) The feasible regions of the two parameters of the LSSVR model are set as $C \in [0, 1 \times 10^3]$, and $\sigma \in [0, 500]$.
(2) In the BPNN model, the Trainlm function is used as a training function; the maximum number of trainings is set to 10,000; and the learning efficiency is set to 0.20.
(3) With respect to the parameters of the GA, the population size, *pop_size*, is set to 50; the maximal number of iterations, *gen_max*, is set to 200; the crossover probability p_c, is set to 0.3; and the mutation probability, p_m, is set to 0.2.
(4) With respect to the parameters of the FOA, the population size, *pop_size*, is set to 50; and the maximal number of iterations, *gen_max*, is set to 200.
(5) With respect to the parameters of the BA, the population size, *pop_size*, is set to 50; the maximal number of iterations, *gen_max*, is set to 200; the minimal and maximal values of acoustic frequency are set to $F_{\max} = 1$ and $F_{\min} = -1$; the pulse intensity attenuation coefficient $\gamma = 0.95$; the pulse frequency increase factor $\delta = 0.05$; the maximum pulse frequency $R^0 = 0.75$; and the maximum pulse loudness $A = 0.25$.
(6) With respect to the parameters of the PSO and CCPSO, the size of the particle swarm, *pop_size,* is set to 50; the maximal number of iterations, *gen_max*, is set to 200; the acceleration parameters $c1 = c2 = 2.0$; the hybrid control parameter, *mix_gen*, is set to 0.7; and the population distribution coefficient, *pop_distr*, is set to 0.7.

Since the number of iterations affects the performance of the models, the numbers of iterations of the optimization processes of all compared models are set equal to ensure the reliability of forecasting. In this paper, all forecasting models are constructed using MATLAB 2010a software on a personal computer with an Intel(R) Core(TM) i7 3.4GHz CPU and 4GB RAM.

3.4 Analysis of forecasting precision

To analyze the forecasting performance of the proposed method, the PEM model [1], BPNN model [29], LSSVR-CCPSO model, and PEM&BPNN model (with PEM to forecast the periodic term and BPNN to forecast the residual term) are considered as contrasting methods.

The well-trained PEM, BPNN, LSSVR-CCPSO, PEM&BPNN, and PEM&LSSVR-CCPSO models are obtained using the training dataset. In Example I, the parameter combination of the LSSVR model that is determined by CCPSO is (46, 59). In Example II, the parameter combination of the LSSVR model that is determined by CCPSO is (25, 78). These trained models are further used to forecast the SMTS value. Figures 4 and 5 plot the forecasting curves of the aforementioned five models and the actual values. Tables 1 and 2 present the indices of forecasting accuracy for the proposed PEM&LSSVR-CCPSO model and the other models.

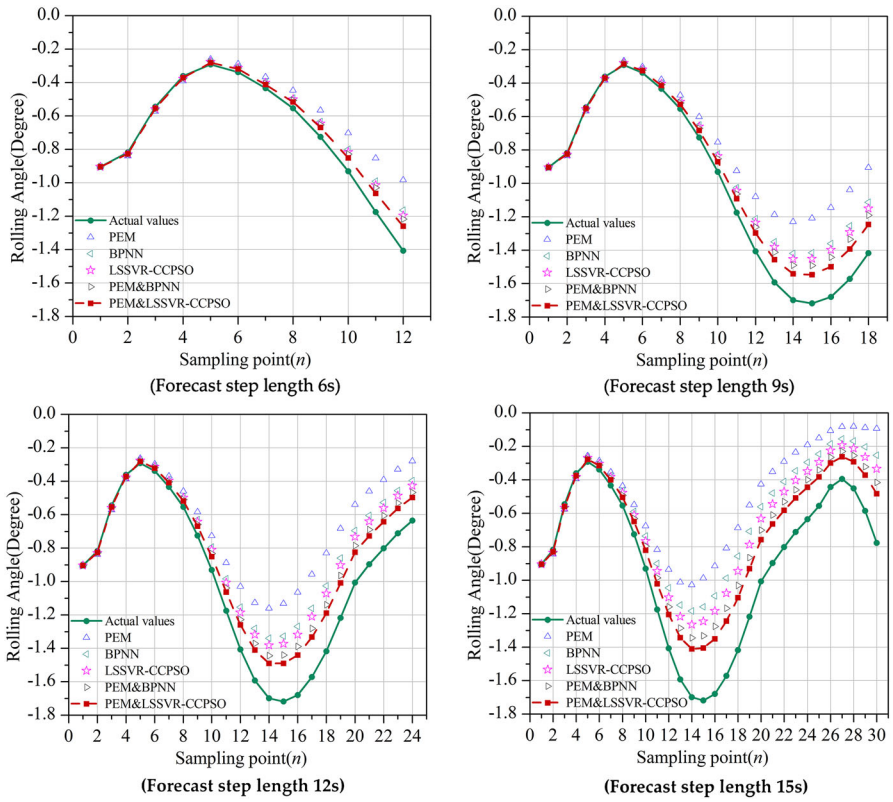

Fig. 4 Forecasting values of EM&LSSVR-CCPSO model and other compared models for Example I

The results in Figs. 4 and 5 demonstrate that the proposed PEM&LSSVR-CCPSO model yields forecasts that are closer to the actual SMTS values than are obtained using the alternative models. The RMSE and MAPE of the proposed PEM&LSSVR-CCPSO model are 0.0623, 0.1036, 0.1463, and 0.1998 and 5.26, 6.08, 10.92, and 18.92 in Example I, and 0.2792, 0.2644, 0.3240, and 0.7304 and 6.18, 7.12, 12.46, and 20.96 in Example II, which are all smaller than those of the other four models in Tables 1 and 2. These results indicate that the proposed approach provides improved SMTS forecasting accuracy. The detail results are analyzed as follows.

First, the forecasts that are provided by the BPNN and LSSVR-CCPSO models are all closer to actual SMTS values than those provided by the PEM model. Therefore, the BPNN and LSSVR-CCPSO models can simulate nonlinear systems of SMTS more accurately than can the PEM model, owing to its advantages in dealing with nonlinear problems. Second, the forecasting accuracy of the LSSVR-CCPSO model is superior to that of the BPNN model, revealing that the LSSVR-CCPSO model is better for nonlinear simulation, including for SMTS forecasting. Furthermore, the RMSE and MAPE for the PEM&BPNN and PEM&LSSVR-CCPSO models are smaller than those for the BPNN and LSSVR-CCPSO models. Therefore, using the PEM for initial forecasting and the BPNN and LSSVR-CCPSO models for residual forecasting better captures the periodicity and nonlinearity of SMTS, favoring its simulation. Finally, Tables 1 and 2 indicate that the RMSE and MAPE of the PEM&LSSVR-CCPSO model forecast series are smaller than those of the PEM&BPNN forecast series, revealing that, in hybrid forecasting, with greater nonlinear fitting ability than the BPNN model, the LSSVR-CCPSO models can better simulate the residual term, so the PEM&LSSVR-CCPSO model yields more accurate predictions than the PEM&BPNN model. Therefore, the attempt to use the PEM to forecast the periodic term of the SMTS and to use the LSSVR-CCPSO algorithm to forecast the residual term of the SMTS feasibly improves the accuracy of prediction of the SMTS.

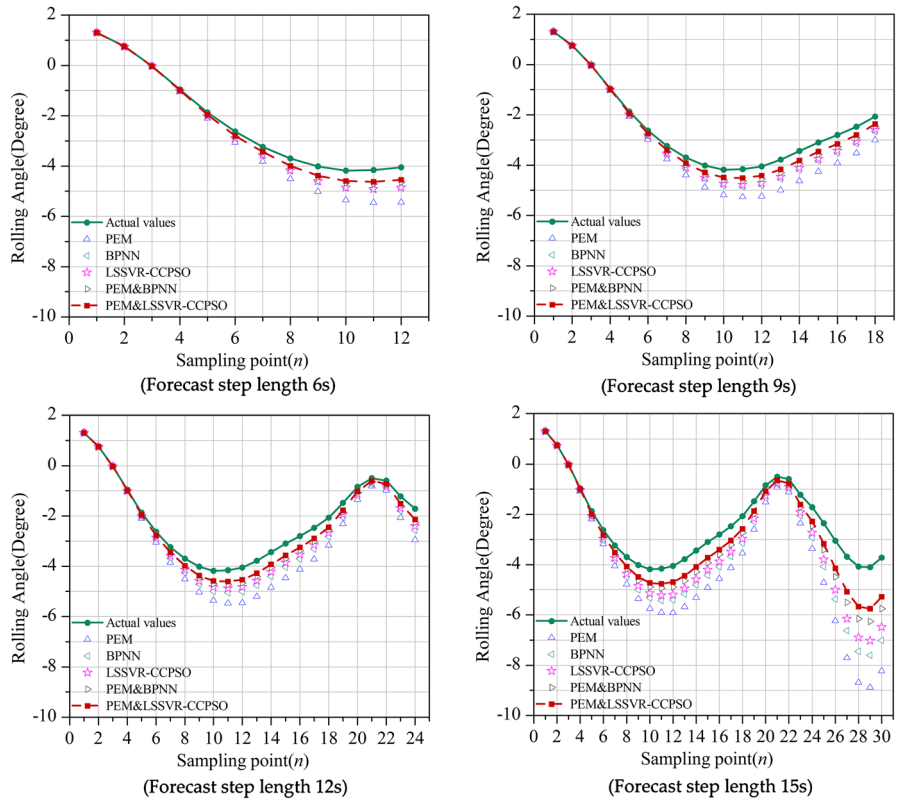

Fig. 5 Forecasting values of EM&LSSVR-CCPSO model and other compared models for Example II

Table 1 Forecasting indexes of PEM&LSSVR-CCPSO model and alternative compared models for Example I

Indexes	RMSE				MAPE (%)			
Forecast step length	6 (s)	9 (s)	12 (s)	15 (s)	6(*s*)	9(*s*)	12 (s)	15 (s)
PEM	0.1783	0.3078	0.3758	0.4650	15.04	18.04	28.04	44.04
BPNN	0.1022	0.1834	0.2512	0.3564	8.63	10.75	18.75	33.75
LSSVR-CCPSO	0.0893	0.1617	0.2208	0.3007	7.54	9.48	16.48	28.48
PEM & BPNN	0.0803	0.1368	0.1778	0.2457	6.78	8.02	13.27	23.27
PEM&LSSVR-CCPSO	0.0623	0.1036	0.1463	0.1998	5.26	6.08	10.92	18.92

Based on the above results, the accuracy in Example II is significantly lower than that in Example I. The sea conditions in Example II are more complicated than in Example I, so the nonlinearity of the ship motion time series is greater. Like that of the existing forecasting models, the forecasting accuracy of the proposed forecasting model decreases as the complexity of the ship motion time series increases. Therefore, the proposed forecasting model remains limited. Unfortunately, the data in the ship motion time series under extreme sea conditions were not properly collected, so the accuracy of the proposed forecasting model under extreme sea conditions cannot be quantified. Therefore, the only conclusion that can be drawn is that the proposed forecasting model is suitable for forecasting ship motion under normal sea conditions. The practicality of the proposed forecasting model under extreme sea conditions deserves further in-depth exploration.

Finally, to test the superiority of the proposed PEM&LSSVR-CCPSO model in forecasting of SMTS over other models, the Wilcoxon signed-rank test was performed. The one-tailed test was conducted

Table 2 Forecasting indexes of PEM&LSSVR-CCPSO model and other compared models for Example II

Indexes	RMSE				MAPE (%)			
Forecast step length	6 (s)	9 (s)	12 (s)	15 (s)	6(*s*)	9(*s*)	12 (s)	15 (s)
PEM	0.7774	0.8427	0.9411	2.1147	17.18	22.68	36.18	60.68
BPNN	0.4617	0.5324	0.6458	1.5449	10.21	14.33	24.83	44.33
LSSVR-CCPSO	0.4490	0.4707	0.5181	1.2936	9.93	12.67	19.92	37.12
PEM&BPNN	0.3308	0.3551	0.4112	0.9517	7.32	9.56	15.81	27.31
PEM&LSSVR-CCPSO	0.2792	0.2644	0.3240	0.7304	6.18	7.12	12.46	20.96

Table 3 Results of Wilcoxon signed-rank test

The significant level		$\alpha = 0.05$			
Forecast step length Critical value to the significant level		6 (s) $T_{0.05} = 17$	9 (s) $T_{0.05} = 47$	12 (s) $T_{0.05} = 91$	15 (s) $T_{0.05} = 151$
Example I	PEM&LSSVR-CCPSO versus PEM	9.27^{T}	8.36^{T}	6.45^{T}	3.52^{T}
	PEM&LSSVR-CCPSO versus BPNN	14.16^{T}	13.24^{T}	11.36^{T}	8.43^{T}
	PEM&LSSVR-CCPSO versus LSSVR-CCPSO	14.67^{T}	13.58^{T}	11.67^{T}	8.57^{T}
	PEM&LSSVR-CCPSO versus PEM&BPNN	16.89^{T}	15.78^{T}	13.39^{T}	10.28^{T}
Example II	PEM&LSSVR-CCPSO versus PEM	8.82^{T}	8.09^{T}	6.05^{T}	3.24^{T}
	PEM&LSSVR-CCPSO versus BPNN	13.90^{T}	12.87^{T}	10.96^{T}	8.10^{T}
	PEM&LSSVR-CCPSO versus LSSVR-CCPSO	14.36^{T}	13.17^{T}	11.36^{T}	8.13^{T}
	PEM&LSSVR-CCPSO versus PEM&BPNN	16.53^{T}	15.53^{T}	12.97^{T}	10.02^{T}

^{T}Denotes that the PEM&LSSVR-CCPSO model significantly outperforms the other alternative compared models

with a significance level of $\alpha = 0.05$. Table 3 presents the test results, which demonstrate that the proposed PEM&LSSVR-CCPSO model significantly outperformed the other models in forecasting.

3.5 Analysis of robustness

To analyze the variation of the forecasting performance of the proposed forecasting model with the different forecasting step, examples of its application are considered. The curve of the variation of the forecasting error, MAPE, of the proposed model is plotted. Figures 6 and 7 plot the forecasting error curves for the two examples.

Figures 6 and 7 demonstrate that the forecasting accuracies of the five used models in Examples I and II decreased with as the forecasting time step increased. The decrease in the forecasting accuracy of the proposed model is obviously less than that of the other four models, indicating that the proposed model is more effective for nonlinear simulation owing to the use of the LSSVR-CCPSO algorithm, so its forecasting accuracy decreases more slowly than those of the other models as the of forecasting time step increases.

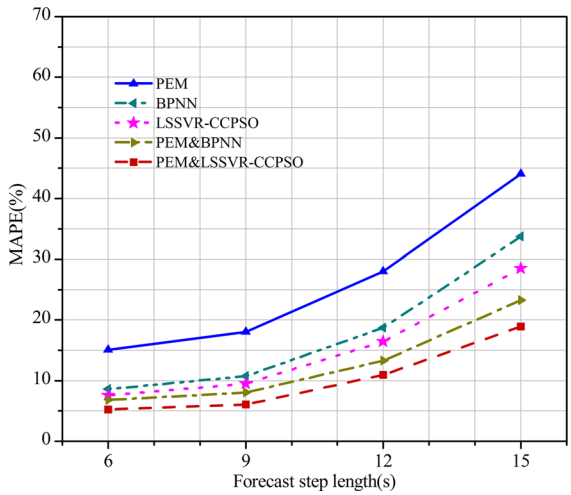

Fig. 6 The error characteristic curves for Example I

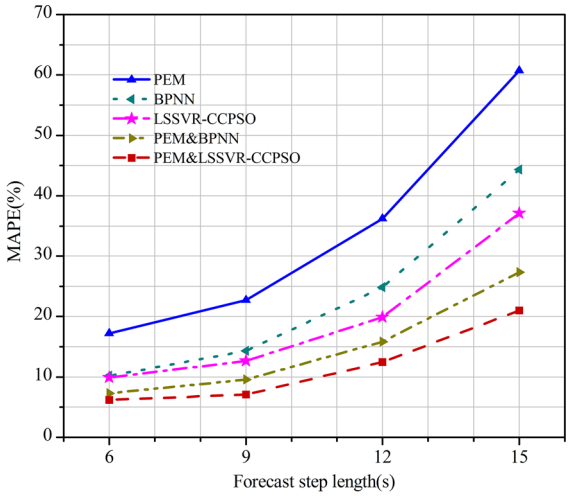

Fig. 7 The error characteristic curves for Example II

In Example II, the ship is slower, and the sea condition is worse, so the problem of ship motion forecasting is more complicated. Consequently, as the forecasting length increases, the increase in the forecasting errors of the selected models is all larger than in Example I, revealing that the forecasting accuracies of the forecasting models all decline as the problem complexity increases. The increase in forecasting error of the proposed model is obviously smaller than that of other models, especially in Example II, which has with more complicated characteristics, indicating that the use of the LSSVR model and the CCPSO algorithm in the PEM&LSSVR-CCPSO model improves its ability to deal with complex problems, its stability and its universality.

With regard to the evaluation of the complexity of the proposed forecasting model, the main steps in ship motion forecasting are as follows: (1) training the PEM; (2) optimizing the parameters of the LSSVR model; (3) training the LSSVR model; (4) forecasting by the PEM; (5) forecasting using the LSSVR model; and (6) calculating the final forecasting value. Among them, the former three steps [(1) to (3)] belong to the model updating stage and the latter three steps [(4) to (6)] are in the model forecasting stage. In this investigation, the total operating time for the later three steps is approximately 5.7 s, which is less than the minimum required operating time of 6 s (the minimum forecast step length in this paper is 6 s). Of the first three steps, step (2) is more time-consuming than steps (1) and (3), which also determines the total operating time for model updating. However, the rolling forecasting process is used, in which model updating and forecasting are performed simultaneously; after the model is updated, forecasting is performed using the updated model. In this paper, the CCPSO algorithm is used to optimize the parameters of the LSSVR model, whose maximum operating time is 42.3 s with 50 instances of parameter optimization. Therefore, based on the minimum forecast step length of 6 s, the forecasting model is updated every eight times steps (4) and (5) are performed. Therefore, the online rolling forecasting of a ship motion time series can be achieved.

3.6 Analysis of optimization performance

To analyze feasibility and superiority of using the CCPSO algorithm to determine the parameters of the LSSVR model, four other commonly used algorithms, GA [18], PSO [17], FOA [20], and BA [30] are used in comparative experiments. The SMTS data in Example I (15s) and Example II (15s) are used in the experiments. Owing to their randomness, evolutionary algorithms are used to optimize the model parameters 50 times. The average number of iterations till convergence, the rate of convergence, and the mean value of the best fitness that is achieved using each model in 200 iterations are calculated.

The average number of iterations is defined as the average number of iterations at convergence over 50 times of the model. The PSO algorithm is used to optimize the parameters of the LSSVR model 50 times, and then the average best fitness is taken as the convergent goal. If the fitness at convergence is equal to or better than the convergent goal, then it is considered to be successful, and the number of successes is increased by one. By this method, the number of successes out of 50 attempts is determined. The rate of convergence is defined as the number of successes divided by 50. Table 4 presents the statistical results.

Table 4 shows that average numbers of iterations at convergence of the proposed algorithm in the two examples are 32 and 36, respectively—fewer than those of the other four algorithms, revealing that the proposed algorithm has a higher search efficiency in each iteration. The rates of convergence of the proposed algorithm in the two examples are 85% and 80%, respectively, as indicated in Table 4

Table 4 The statistical results of performance criteria

Example	Algorithms	The average iteration of convergence	The rate of convergence (%)	The mean value of the best fitness
Example I (step length 15 (s))	GA	61	67	13.42
	PSO	67	62	13.78
	FOA	85	55	14.32
	BA	89	58	14.18
	CCPSO	32	85	12.28
Example II (step length 15 (s))	GA	70	61	17.86
	PSO	75	56	18.23
	FOA	89	51	19.45
	BA	94	53	19.21
	CCPSO	36	80	15.43

exceeding those of the other four algorithms, revealing that the proposed algorithm exhibits less random fluctuation and greater stability in the optimization of the parameters of the LSSVR model, favoring its forecasting accuracy. The mean values of the best fitness that is achieved using the proposed algorithm in the two examples are 12.28 and 15.43, respectively, which are considerably smaller than those obtained using the other four algorithms. Therefore, the search efficiency of proposed algorithm exceeds those of the other four algorithms, revealing its great advantage in solving SMTS forecasting problems. Therefore, using the CCPSO algorithm to determine the parameters of the LSSVR model to improve is accuracy in forecasting SMTS is feasible.

In this paper, the CCPSO algorithm is used to optimize the parameters of the LSSVR model, which only solves the parameter updating problem in the modeling processes. In fact, there are many existed optimization algorithms, and more feasible ones are being proposed, thus, it is unable to completely compare with these algorithms. The improved CCPSO algorithm in this paper has been demonstrated only to be superior to the considered classical optimization method, and the authors cannot guarantee that the CCPSO algorithm is the very best of all algorithms for the intended purpose. Optimization of the parameters of the LSSVR model warrants further exploration to further improve its forecasting accuracy.

4 Conclusions

The accurate and rapid forecasting of SMTS is very important for ship stability and the efficient operation of the equipment on board. Therefore, the development of a new model for accurately forecasting SMTS is valuable. In this investigation, the PEM, the LSSVR model, and the CCPSO algorithm were combined in a PEM&LSSVR-CCPSO model for forecasting SMTS. The proposed model was evaluating for use in forecasting the SMTS of two ships sailing on the ocean. The results of a numerical test demonstrated that the proposed model outperformed PEM, BPNN, and LSSVR models in forecasting SMTS. Dividing the SMTS into a periodic term and a nonlinear term, using the PEM to forecast the periodic term and the LSSVR model to forecast the nonlinear term by forecasting the residual term that was generated by the PEM, enhanced the ability to deal with periodicity and strong nonlinearity of SMTS. Moreover, the introduction of the CCPSO algorithm to determine the parameters of the LSSVR model strengthened the effectiveness of the LSSVR model in linear simulation, further improving the forecasting accuracy of the PEM&LSSVR-CCPSO model. Each component of the proposed hybrid forecasting approach improved forecasting accuracy. Therefore, the favorable results herein indicated that the proposed model forecasts SMTS with greater accuracy than other models.

The improved PEM has greater periodicity processing ability than the traditional PEM, but this investigation focused only on a PEM with an advanced nonlinear

model to improve forecasting performance, and only the traditional PEM was used to establish the mixed forecasting model. Thus, a hybrid forecasting model that is based on an improved PEM and an advanced nonlinear forecasting model deserves further exploration. Ship motion has strong time-varying characteristics; the newer the data used in the training model are, the higher the forecasting accuracy of the forecasting model is. Therefore, the updating speed of a forecasting model important affects forecasting accuracy. Accordingly, a hybrid forecasting method that is based on the periodic graph method and an online LSSVR model should be investigated. Fast and accurate determination of the parameters of the LSSVR model determines its updating speed and forecasting accuracy. To improve further the forecasting accuracy, more efficient parameter optimization methods should be developed.

Acknowledgements The work is supported by the following project grants, National Natural Science Foundation of China (51509056); Heilongjiang Province Natural Science Fund (E2017028); Fundamental Research Funds for the Central Universities (HEUCFG201813); Open Fund of the State Key Laboratory of Coastal and Offshore Engineering (LP1610); Heilongjiang Sanjiang Project Administration Scientific Research and Experiments (SGZL/KY-08); and Jiangsu Normal University (No. 9213618401), China.

Author contributions M-WL and W-CH conceived and designed the experiments; JG and LZ performed the experiments; M-WL and W-CH analyzed the data and wrote the paper.

Compliance with ethical standards

Conflict of interest The authors declare that they have no conflict of interest.

References

1. Peng, X.Y., Yan, J.S., Qiu, D.Q.: Study of ship motion modeling and prediction based on periodogram methods. Ship Eng. **33**(5), 60–64 (2011). https://doi.org/10.13788/j.cnki.cbgc.2011.05.020
2. Sun, H.F., Peng, X.Y., Zhao, X.R.: An improved periodogram algorithm with application in ship motion forecasting. J. Harbin Eng. Univ. **29**(11), 1181–1184 (2008)
3. Shen, J.H.: GM (1, 1) for modeling oscillation series via triangle transformation. J. Grey Syst. **14**, 5–8 (2002)
4. Liu, L.S., Peng, X.F.: Second order gray neural network in ship roll forecast. J. Ship Mech. **15**, 468–472 (2011)
5. Yumori, I.R.: Real time prediction of ship response to ocean waves using time series analysis. IEEE Oceans **81**, 1082–1089 (1981). https://doi.org/10.1109/OCEANS.1981.1151574
6. Zhang, Y.S., Zhou, L.X., Cai, F., Shi, A., Yang, B.: A new technology of forecasting the takeoff/touchdown opportunity of ship-born helicopter in heavy sea. Navig. China **53**, 5–10 (2002)
7. Zhao, X.R., Peng, X.Y., Lu, S.P., Wei, N.X.: Extreme short prediction of big ship motion having wave survey. J. Ship Mech. **7**(2), 39–44 (2003)
8. Peng, X.Y., Liu, C.D.: Extreme short time prediction of ship motion based on lattice recursive least square. J. Ship Mech. **16**, 44–51 (2012)
9. Khan, A., Bil, C., Marion, K.E.: Ship motion prediction for launch and recovery of air vehicles. Proc. MTS/IEEE OCEANS **3**, 2795–2801 (2005). https://doi.org/10.1109/OCEANS.2005.1640198
10. Gu, M., Liu, C.D., Zhang, J.F.: Extreme short-term prediction of ship motion based on chaotic theory and RBF neural network. J. Ship Mech. **17**(10), 1147–1152 (2013)
11. Shen, Y., Xie, M.P.: Ship motion short time modeling and prediction based on RNN. Chin. J. Sci. Instrum. **25**(4), 977–978 (2004)
12. Xu, P., Jin, H.Z., Wang, K.J., Yan, L.T.: New method of ship rolling real time forecast. Shipbuild. China **43**(1), 70–74 (2002)
13. Cao, J., Cai, A.: A robust shot transition detection method based on support vector machine in compressed domain. Pattern Recognit. Lett. **28**(12), 1534–1540 (2007). https://doi.org/10.1016/j.patrec.2007.03.011
14. Vapnik, V., Golowich, S., Smola, A.: Support vector machine for function approximation regression estimation and signal processing. Adv. Neural Inf. Process. Syst. **9**, 281–287 (1996)
15. Hong, W.C., Dong, Y., Chen, L.Y., Wei, S.Y.: SVR with hybrid chaotic genetic algorithms for tourism demand forecasting. Appl. Soft Comput. **11**(2), 1881–1890 (2011). https://doi.org/10.1016/j.asoc.2010.06.003
16. Hong, W.C., Dong, Y., Zheng, F., Lai, C.Y.: Forecasting urban traffic flow by SVR with continuous ACO. Appl. Math. Model. **35**(3), 1282–1291 (2011). https://doi.org/10.1016/j.apm.2010.09.005
17. Geng, J., Li, M.W., Dong, Z.H., Liao, Y.S.: Port throughput forecasting by MARS-RSVR with chaotic simulated annealing particle swarm optimization algorithm. Neurocomputing **147**, 239–250 (2015). https://doi.org/10.1016/j.neucom.2014.06.070
18. Kang, H.G., Li, M.W., Zhou, P.F., Zhao, Z.H.: Prediction of passenger traffic volume using ν-support vector regression optimized by chaos adaptive genetic algorithm. J. Dalian Univ. Technol. **52**(2), 227–232 (2012)
19. Li, M.W., Hong, W.C., Kang, H.G.: Urban traffic flow forecasting using Gauss-SVR with cat mapping, cloud model and PSO hybrid algorithm. Neurocomputing **99**, 230–240 (2013). https://doi.org/10.1016/j.neucom.2012.08.002
20. Li, M.W., Geng, J., Han, D.F., Zheng, T.J.: Ship motion prediction using dynamic seasonal Rv-SVR with phase space reconstruction and the chaos adaptive efficient FOA. Neurocomputing **174**, 661–680 (2016). https://doi.org/10.1016/j.neucom.2015.09.089
21. Geng, J., Huang, M.L., Li, M.W., Hong, W.C.: Hybridization of seasonal chaotic cloud simulated annealing algorithm in a SVR-based load forecasting model. Neurocomputing **151**,

1362–1373 (2015). https://doi.org/10.1016/j.neucom.2014.10.055
22. Chai, R., Tsourdos, A., Savvaris, A., Chai, S., Xia, Y.: Two-stage trajectory optimization for autonomous ground vehicles parking maneuver. IEEE Trans. Ind. Inf. https://doi.org/10.1109/TII.2018.2883545 (**in press**)
23. Chai, R., Savvaris, A., Tsourdos, A., Xia, Y.: An interactive fuzzy physical programming for solving multiobjective skip entry problem. IEEE Trans. Aerosp. Electron. Syst. **53**(5), 2385–2398 (2017). https://doi.org/10.1109/TAES.2017.2696281
24. Chai, R., Savvaris, A., Tsourdos, A., Chai, S., Xia, Y.: Unified multiobjective optimization scheme for aeroassisted vehicle trajectory planning. J. Guid. Control Dyn. **41**(7), 1521–1530 (2018). https://doi.org/10.2514/1.G003189
25. Li, M.W., Kang, H., Zhou, P., Hong, W.C.: Hybrid optimization algorithm based on chaos, cloud and particle swarm optimization algorithm. J. Syst. Eng. Electron. **24**(2), 324–334 (2013)
26. Suykens, J.A.K., Vandewalls, J.: Least squares support vector machine classifiers. Neural Process. Lett. **9**(3), 293–300 (1999). https://doi.org/10.1023/A:1018628609742
27. Deng, N., Tian, Y., Zhang, C.: Support Vector Machines: Optimization Based Theory, Algorithms, and Extensions. CRC Press, Boca Raton (2012)
28. Liu, H., Zhou, Y.: A cloud adaptive particle swarm optimization algorithm based on mean. Comput. Eng. Sci. **33**(5), 97–101 (2011)
29. Luo, W.L., Zhang, Z.C.: Modeling of ship maneuvering motion using neural networks. J. Mar. Sci. Appl. **15**, 426–432 (2016). https://doi.org/10.1007/s11804-016-1380-8
30. Yang, X.S.: A new metaheuristic bat-inspired algorithm. In: González, J.R., Pelta, D.A., Cruz, C., Terrazas, G., Krasnogor, N. (eds.) Nature Inspired Cooperative Strategies for Optimization, vol. 284, pp. 65–74. Springer, Heidelberg (2010). https://doi.org/10.1007/978-3-642-12538-6_6

Publisher's Note Springer Nature remains neutral with regard to jurisdictional claims in published maps and institutional affiliations.